

Impact of Obesity on the CCR6-CCL20 Axis in Epidermal $\gamma\delta$ T Cells and IL-17A Production in Murine Wound Healing and Psoriasis

Running Title: CCR6⁺ and IL-17A⁺ Epidermal $\gamma\delta$ T Cells during Obesity

William Lawler, Tanya Castellanos, Emma Engel, Cristian R. Alvizo, Antolette Kasler, Savannah Bshara-Corson, and Julie M. Jameson

*Department of Biological Sciences, California State University San Marcos, San Marcos, CA 92096

Corresponding Author: Dr. Julie Jameson, Department of Biological Sciences, California State University San Marcos, 333 S. Twin Oaks Valley Rd., San Marcos, CA 92096. Phone: (760) 750-8274 Email Address: jjameson@csusm.edu

Support of Work:

This work was supported by NIHR15DK127440.

Abbreviations: IMQ, Imiquimod; ILC, innate lymphoid cell; MAIT, mucosal-associated invariant T; TCR, T cell receptor; scRNAseq, single-cell RNA sequencing; HFD, high fat diet; NCD, normal chow diet; DEG, differentially expressed gene; DC, dendritic cell; NK, natural killer cell; NMD, nonsense-mediated decay; WD, wounded; NKT, natural killer T cell.

Abstract

Obesity is associated with comorbidities including type 2 diabetes, chronic nonhealing wounds and psoriasis. Normally skin homeostasis and repair is regulated through the production of cytokines and growth factors derived from skin-resident cells including epidermal $\gamma\delta$ T cells. However epidermal $\gamma\delta$ T cells exhibit reduced proliferation and defective growth factor and cytokine production during obesity and type 2 diabetes. One of the genes modulated in epidermal $\gamma\delta$ T cells during obesity and type 2 diabetes is CCR6, which is the receptor for CCL20. CCL20 is elevated in the skin during obesity and type 2 diabetes. Here we identify a subset of murine epidermal $\gamma\delta$ T cells that expresses CCR6 in response to activation *in vitro* and post-wounding or psoriasis induction with imiquimod *in vivo*. We show that CCL20 stimulates epidermal $\gamma\delta$ T cells to produce IL-17 suggesting CCR6 regulates the IL-17 axis as in dermal $\gamma\delta$ T cells. Further, epidermal $\gamma\delta$ T cells upregulate CCR6 and produce IL-17 during murine models of wound repair and psoriasis. Obesity increases CCR6 and IL-17 expression by epidermal $\gamma\delta$ T cells during wound repair but has less of an effect during psoriasis. These findings have novel implications for the regulation of a specific population of IL-17-producing epidermal $\gamma\delta$ T cells during skin damage and inflammation.

Introduction

Obesity is correlated with increases in skin comorbidities including chronic nonhealing wounds and psoriasis (1–4). Chronic nonhealing wounds affect 2.5% of the US population while psoriasis affects 8 million Americans (1, 5). Normally the skin provides a protective barrier from mechanical, chemical, and pathogenic external threats. The TNF- α -IL-17 axis provides antimicrobial roles and induces keratinocyte proliferation and neutrophil responses in wound repair (6, 7). However, dysregulation of the TNF- α -IL-17 axis caused by obesity alters the cellular composition and function in the skin resulting in premature keratinocyte differentiation, altered skin-resident T cell number and function, and increased barrier permeability (7, 8). All of these factors negatively impact chronic nonhealing wounds and psoriasis (1).

Alterations in TNF- α and IL-17 production during chronic nonhealing wounds and psoriasis have been attributed to dermal $\gamma\delta$ T cells, dermal Th17 $\alpha\beta$ T cells, innate lymphoid cells (ILC), and mucosal-associated invariant T (MAIT) cells (9–12). In contrast, resident epidermal $\gamma\delta$ T cells, also known as dendritic epidermal T cells (DETC), have been largely considered bystanders and not active IL-17 producers (13). Epidermal $\gamma\delta$ T cells bear the V γ 5V δ 1 TCR and are rapidly activated by stressed or damaged keratinocytes to release cytokines, chemokines, and growth factors including TNF- α and in some cases IL-17A (14–16). In lean mice, epidermal $\gamma\delta$ T cells serve as critical players in skin homeostasis and wound healing (17–20). However, obesity causes a reduction in TNF- α production by epidermal $\gamma\delta$ T cells at the wound site indicating a shift in function (15). Since epidermal $\gamma\delta$ T cells normally act early in wound repair, they may also negatively impact chronic wounds and inflammatory skin disease (13).

One receptor that has been associated with IL-17 producing dermal $\gamma\delta$ T cells (T $\gamma\delta$ 17) is CCR6. The majority of murine dermal V γ 4 and V γ 6 T cells express CCR6, which facilitates recruitment to the epidermis in response to psoriasis-like inflammation (13, 21, 22). CCR6 is also required for efficient wound repair as CCR6^{-/-} mice exhibit delays in wound closure (23). Obese and diabetic patients exhibit elevated CCL20 in the skin, which likely impacts CCR6⁺ T cell recruitment and function(24). Although CCR6 regulates other IL-17-producing T cell populations, epidermal $\gamma\delta$ T cells have not been included as they already reside in the epidermis and do not express CCR6 constitutively (13, 25). Thus, epidermal $\gamma\delta$ T cells may exhibit unique regulation and function of CCR6 especially in obesity.

In this study we identify how epidermal $\gamma\delta$ T cells participate in obesity-related skin complications such as wound healing and psoriasis-like inflammation. We find that CCR6 is expressed by a distinct population of activated epidermal $\gamma\delta$ T cells and CCL20 induces this subset to produce IL-17. Using previously published single cell RNA sequencing (scRNAseq) data, we show that CCR6⁺ epidermal $\gamma\delta$ T cells express IL-17-associated genes during psoriasis-like inflammation. We validate these findings in murine models of wound repair and IMQ-induced psoriasis-like inflammation where CCR6 and/or IL17A are expressed by epidermal $\gamma\delta$ T cells *in vivo*. Obesity increases the number of epidermal $\gamma\delta$ T cells expressing CCR6 and IL-17A during wound healing, which underscores the significant impact of obesity on skewing toward an IL-17 proinflammatory response.

Materials and Methods

Mice

C57BL/6N mice were purchased from Taconic Biosciences (Rensselaer, NY). 16 to 20-week-old male mice were studied for all cell culture and flow cytometry experiments. Male C57BL/6-Il17atm1Bcgen/J mice (JAX stock 018472) were purchased from The Jackson Laboratory (Bar Harbor, Maine). All C57BL/6-Il17atm1Bcgen/J mice used for experiments were purchased between the ages of 4-6 weeks of age and used between 18-24 weeks of age. Mice received access to food and water ad libitum and were housed in the animal facility at California State University San Marcos. For obesity studies, 6 week old male C57BL/6-Il17atm1Bcgen/J mice were fed either a high fat diet (HFD) consisting of 60 kcal% fat diet (D12492, Research Diets) or normal chow diet (NCD) (D12450J, Research Diets) for 12-16 weeks. All experimental procedures involving animals were reviewed and approved by the Institutional Animal Care and Use Committee of California State University San Marcos (21-003).

Epidermal T Cell Culture

Epidermal cells were harvested from the back skin of 16 to 20-week-old wild-type mice as previously described (26). Briefly, the back skin was removed, cut into 1cm² squares, and incubated on 0.3% trypsin-GNK (0.09% glucose, 0.84% sodium chloride and 0.04% potassium chloride) at 37°C with 5.0% CO₂ for 3.5 hours. The epidermis was then peeled from the dermis and shaken in 0.3% trypsin GNK with 0.1% DNase at 37°C for 10 minutes. The cell solution was placed in DMEM with 10% heat inactivated FBS, 2.5% HEPES buffer, 1% 100x non-essential amino acids (NEAA), 1% 100mM sodium pyruvate, 1% penicillin streptomycin glutamine (PSG), vitamins and 0.1% 2-mercaptoethanol (2-ME). The cells were filtered through Sera-Separa filter columns, pelleted, and purified with Lympholyte M prior to culture. The

epidermal cells were plated in a 96-well plate containing RPMI-1640 media with 10% FBS, 2.5% HEPES buffer, 1% NEAA, 1% sodium pyruvate, 1% PSG, 0.1% 2-ME, and 20 U/ml Interleukin 2 (IL-2). 2µg/ml of Concanavalin A (ConA) and 1µg/ml of indomethacin were added at the initiation of cell culture. Twice a week fresh media without ConA and indomethacin was added. Cells were restimulated every 3 weeks with 1µg/ml of ConA and harvested when epidermal $\gamma\delta$ T cells made up over 95% the cells in culture (typically 10 weeks).

Epidermal $\gamma\delta$ T Cell Activation

For *in vitro* studies, 24-well plates were precoated with 1µg/ml or 10µg/ml of anti-CD3ε for 24 hours at 37°C with 5.0% CO₂. The supernatant was harvested and stored at -80°C for Luminex analysis. For intracellular cytokine staining, the cells were stimulated for 6 hours and 5ug/ml Brefeldin A (BFA) was added at hour 2. BD fixation and permeabilization kit (BD Cytofix/Cytoperm) was used per manufacturer's instructions. The following antibodies were used: anti-CD3 (145-2C11), $\gamma\delta$ TCR (GL3), CD25 (3C7) and CCR6 (29-2L17) (Biolegend, San Diego, CA). Flow cytometry was performed on a Accuri C6 (BD Biosciences, San Diego, CA) and data was analyzed with FlowJo software (BD Biosciences).

IMQ Induction of Psoriasis-like Inflammation

5mg of 5% IMQ cream (IMQ Cream 5%, Fougera Pharmaceuticals Inc.) was applied to the right ear and control cream (Vanicream, Pharmaceutical Specialties, Inc.) applied to the left ear of C57BL/6-Il17atm1Bcgen/J mice daily for up to 3 days (9). Mice were individually housed and monitored daily. At the end of the experiment, ears were harvested for staining and immunofluorescent microscopy.

128

129 Wounding Model

130 C57BL/6-Il17atm1Bcgen/J mice between 20-24 weeks of age were anesthetized with a mixture
131 of 1.75L/m O₂ and 2.5% of isoflurane and then received a 2-mm punch biopsy wound on one
132 ear. Mice were individually housed and monitored daily. At 1-3 days post-wounding, the ears
133 were harvested for staining and immunofluorescent microscopy.

134

135 Epidermal Sheet Immunofluorescent Staining and Microscopy

136 Epidermal sheets were prepared as previously described (26). Briefly, ears were split in half and
137 placed on ammonium thiocyanate solution (1x dPBS, 3.6% ammonium thiocyanate) dermis side
138 down, and incubated for 15 minutes, after which the epidermis was peeled from the dermis.
139 Epidermal sheets were floated on 1x dPBS for 5 minutes, then floated on 2 µg/ml anti-Vγ5 and
140 anti-CCR6 (BioLegend, San Diego, CA) for 1 hour at 37°C with 5.0% CO₂. Epidermal sheets
141 were rinsed on 1x dPBS and mounted with Slowfade Gold Antifade Reagent with DAPI
142 (Invitrogen, Waltham, MA). Slides were examined using an immunofluorescent microscope
143 (Nikon DS-Qi2, Nikon, Tokyo, JPN). Expression of IL-17A (GFP), CCR6 (PE), and the γδTCR
144 (APC) were examined at the site of wounding or psoriasis induction. Images were captured using
145 NIS-Element D 4.1300 64 program (Melville, NY) at original magnification x200, and processed
146 using Adobe Photoshop 2022 (San Jose, CA). Total epidermal γδ T cell number, as well as the
147 number of epidermal γδ T cells that expressed CCR6, and/or IL-17 were quantified and then
148 calculated as cells/mm². In both the psoriasis and wounding experiments, a total of 7 regions
149 were photographed per epidermal sheet per ear, accounting for both wounded and non-wounded
150 ears, as well as Imiquimod-treated and untreated control ears. Each ear provided two epidermal

151 sheets. In total 672 images were captured, analyzed and quantified between the Imiquimod and
152 wounding models.

153 154 sc-RNA Sequencing Data Processing and Analysis

155 Publicly available scRNA seq data was downloaded as fastq files from the NIH Gene
156 Expression Omnibus (GEO) database (GSE149121) (20). Files were downloaded to the Linux
157 terminal and transferred to the Cellranger Analysis Pipeline terminal. The study by Liu, et al.
158 2020 used single cell transcriptomics of CD45⁺ cells from mice treated with IMQ for 7 days
159 (20). All fastq files were individually run through Cellranger Analysis Pipelines v6.1 (10x
160 Genomics) to perform gene quantification and sequence alignment to the 10x Genomics mouse
161 reference genome (mm10). Additionally, Cellranger was utilized to subsample experiment reads
162 and produce an aggregated gene expression matrix. Once aggregation and structuring of the data
163 was completed, Cellranger generated a cloupe file that was uploaded to the visualization
164 software Loupe Browser v6.0 (10x Genomics) to be used for downstream analysis of scRNAseq
165 data. scRNAseq data was then uploaded to Loupe Browser for further analysis. Epidermal $\gamma\delta$ T
166 cell populations were identified by their expression of *Tcr α -v5*, *Fc ϵ r1g* and *CD3*. Any
167 contaminating non epidermal $\gamma\delta$ T cell populations were eliminated based on their positive
168 expression of *Cd4*, *Cd8*, *Tcr α -v4*, *Tcr α -v6*, *Krt5*, *Krt10*, *Cd207* or *Lyz1*. Once the epidermal $\gamma\delta$ T
169 cell clusters were identified, further analysis was performed by clustering the epidermal $\gamma\delta$ T
170 cells into subsets (CCR6⁺IMQ, CCR6⁺control, CCR6⁻IMQ, CCR6⁻control). Subsets were
171 compared between IMQ treated and untreated control mice and differentially expressed genes
172 (DEGs) were exported from Loupe Browser and submitted to Ingenuity Pathway Analysis (IPA)
173 (Qiagen) for core analysis.

174

175 Statistical Analysis

176 Unpaired Student t-tests and z-test were used to analyze T cell numbers and corresponding
177 cytokine production. All statistical tests performed using Prism Graph Pad software (Dotmatics,
178 Boston, MA). All findings are considered significant at $p < 0.05$. Log2-fold change in Loupe
179 Browser was calculated by using the localized ratio of normalized mean gene UMI counts in
180 each cluster relative to all other clusters.

181

182 **Results**

183 CCR6 is upregulated by a subset of epidermal $\gamma\delta$ T cells upon anti-CD3 stimulation.

184 Epidermal $\gamma\delta$ T cells do not express CCR6 on the cell surface during homeostatic
185 conditions (25). While resting epidermal $\gamma\delta$ T cells do not express CCR6, we tested whether
186 CCR6 is expressed upon activation. Epidermal $\gamma\delta$ T cell lines were stimulated with or without
187 anti-CD3 stimulation for 24 hours and CCR6 expression was examined by flow cytometry. Live,
188 V γ 5 TCR⁺ cells were gated and analyzed for CCR6 expression. Upon stimulation with anti-CD3
189 for 24 hours, a subset of epidermal $\gamma\delta$ T cells express CCR6 and CD25 (Fig. 1A). Of note is the
190 role that may be played by IL-2 in the CCR6-expressing population.

191 CCL20 increases IL-17A, but not TNF- α production by activated epidermal $\gamma\delta$ T cells

192 Previous studies show that CCR6⁺ dermal V γ 4 T cells secrete IL-17A in response to skin
193 damage and during psoriasis (13, 16, 27). Lower levels of IL-17A have also been detected by
194 epidermal $\gamma\delta$ T cells during wound repair and contact hypersensitivity, but it is unknown if this is
195 regulated by CCL20 and whether this is a distinct population (15, 16). To determine whether IL-

17A and TNF- α production by epidermal $\gamma\delta$ T cells is augmented by the CCR6 ligand, CCL20, we examined epidermal $\gamma\delta$ T cells post-stimulation with CCL20 and/or anti-CD3. There is not a significant increase in epidermal $\gamma\delta$ T cells producing IL-17A post-stimulation with anti-CD3, but there is a significant increase in epidermal $\gamma\delta$ T cells producing TNF- α (Fig. 1B). CCL20 alone does not increase the percent of epidermal $\gamma\delta$ T cells producing either IL-17A or TNF- α . Furthermore, CCL20 administered with anti-CD3 stimulation does not induce more epidermal $\gamma\delta$ T cells to produce TNF- α than anti-CD3 alone (Fig. 1B). However, CCL20 administered with anti-CD3 stimulation significantly increases the percent of epidermal $\gamma\delta$ T cells producing IL-17A. Interestingly, upon the addition of anti-CD3 and CCL20, there are four functional subsets of epidermal $\gamma\delta$ T cells: TNF- α^- /IL-17A $^-$, TNF- α^+ /IL-17A $^-$, TNF- α^- /IL-17A $^+$ and TNF- α^+ /IL-17A $^+$. This challenges previous studies suggesting that epidermal $\gamma\delta$ T cells are preprogrammed away from a T $\gamma\delta$ 17 fate.

Epidermal $\gamma\delta$ T cells expressing CCR6 exhibit a unique gene expression profile

To examine gene expression by CCR6 $^+$ epidermal $\gamma\delta$ T cells during psoriasis, publicly available scRNAseq data from Liu et. al was reanalyzed with a focus on CCR6 $^+$ or CCR6 $^-$ epidermal $\gamma\delta$ T cells (20). In this study RNA was isolated from C57BL/6J mouse skin treated with or without 5% Imiquimod for seven days and scRNAseq was performed. The authors report a cluster of epidermal $\gamma\delta$ T cells in a t-distributed stochastic neighbor embedding (t-SNE) plot indicating a broad population with a potential for subsets of epidermal $\gamma\delta$ T cells with differing gene expression. To specifically analyze epidermal $\gamma\delta$ T cells, target cells were sorted from the overall cell count using Loupe Browser based on well-established marker genes ($Cd3^+$, $Tcr\gamma-v5^+$, $Trdc^+$, $Cd4^-$, $Cd8^-$). Minor populations of contaminant keratinocytes and Langerhans cells were

excluded by removing cells exhibiting high levels of *Krt5*, *Krt10* and *Krt14* for the keratinocytes and high levels of *Cd207* for the Langerhans cells, yielding a total of 236 epidermal $\gamma\delta$ T cells for analysis (Fig. 2A). These exclusions produced three distinct epidermal $\gamma\delta$ T cell populations (labeled cluster 1-3 in Fig. 2A).

Epidermal $\gamma\delta$ T cells were further clustered based on treatment group and CCR6 expression (CCR6⁺IMQ, CCR6⁺control, CCR6⁻IMQ, CCR6⁻control) (Fig. 2A). Prior to IMQ treatment, CCR6⁻ epidermal $\gamma\delta$ T cells are represented in clusters 1, 2 and 3. However, post-IMQ treatment the CCR6⁻ epidermal $\gamma\delta$ T cells have predominantly centralized to cluster 2. Pre-IMQ treatment CCR6⁺ epidermal $\gamma\delta$ T cells are represented in cluster 3, while post-treatment the CCR6⁺ epidermal $\gamma\delta$ T cells are represented in both cluster 2 and cluster 3. A locally distinguishing differential gene expression (DGE) analysis was run between the CCR6⁺ and CCR6⁻ epidermal $\gamma\delta$ T cell populations with and without IMQ treatment and a heat map was generated showcasing the top 10 significantly upregulated genes per cluster based on the logarithmic fold change of gene expression between each group during paired comparison (Fig. 2B).

Interestingly, both CCR6⁺ subsets differentially express the transcription factor *Rora*, which regulates both CCR6 and IL17 expression (Fig. 2B) (28). To better characterize each individual epidermal $\gamma\delta$ T cell population we analyzed DEGs between paired subsets. Comparing the CCR6⁺control and CCR6⁻control groups, we observe that the CCR6⁺control gene profile is more inflammatory, favoring immune cell infiltration (*Ccl1*, *Serpine1*, *Il17f*), whereas the CCR6⁻control group does not exhibit the upregulation of any DEGs above 5-fold. However, when examining gene expression changes exceeding 4-fold, the CCR6⁻control subset demonstrates increased expression of genes related to mitotic cell cycle, DNA binding, and cell motility (*Maff*, *Klf4*) (Fig. 2C top left). Next, in the comparison between CCR6⁺IMQ and CCR6⁻IMQ treatment

groups, the CCR6⁺IMQ subset exhibits a T γ δ 17 inflammatory profile, with a >5-fold upregulation of *Il17f*, along with lower level increases in *Rora*, *IL22*, and *Jaml*. While the CCR6⁻IMQ subset experiences a >3-fold upregulation in genes associated with cytokinesis, proliferation and cell motility (*Tubb2a*, *Fos*, *Plscr1*) (Fig. 2C top right).

In the comparison among CCR6⁺ groups, the CCR6⁺IMQ subset consistently exhibits a pro-inflammatory profile compared to all other subsets, with a greater than 5-fold change in *IL22* expression (Fig. 2C bottom left). On the other hand, the CCR6⁺control subset still shows a >3-fold upregulation in genes associated with immune cell infiltration (*Ccl1*, *Serpine1*). Lastly, the comparison among CCR6⁻ subsets indicate minimal gene upregulation except for potential immune cell recruitment (*Ccl5*) in the CCR6⁻IMQ subset (Fig. 2C bottom right). Our results suggest that CCR6 expressing epidermal $\gamma\delta$ T cells in psoriasis exhibit a skewed IL17 focused response.

Psoriasis increases MYC pathway signaling by CCR6⁺ epidermal $\gamma\delta$ T cells.

IPA core analysis was performed to further elucidate the biological processes and molecular mechanisms that differentiate CCR6⁺ epidermal $\gamma\delta$ T cell subsets in psoriasis. Top differentially expressed genes were clustered into canonical pathways using IPA Knowledge Base platform (Fig. 3A). Comparison of CCR6⁺IMQ to CCR6⁻IMQ subsets revealed Eukaryotic Translation Elongation, Eukaryotic Translation Termination, Response of EIF2AK4 (GCN2) to Amino Acid Deficiency, SRP-dependent Cotranslational Protein Targeting to Membrane, Eukaryotic Translation Initiation, Nonsense-Mediated Decay (NMD), Selenoamino Acid Metabolism, EIF2 Signaling and Major Pathway of rRNA Processing in the Nucleolus and Cytosol as the significantly upregulated pathways of CCR6⁺IMQ subsets in psoriasis when

compared to CCR6⁻IMQ subsets in psoriasis (Fig. 3A). Examination of significantly differentiated upstream regulators between these subsets revealed that the MYC pathway is significantly upregulated within the population of CCR6⁺IMQ epidermal $\gamma\delta$ T cells when compared to CCR6⁻IMQ epidermal $\gamma\delta$ T cells (Fig. 3B). The MYC pathway is predicted by the IPA Knowledge Base to be linked with activation of the transcription factor *Rora* (Fig. 3B). Analysis of the *Rora* downstream pathway shows that upregulation of *Rora* by CCR6⁺IMQ epidermal $\gamma\delta$ T cells directly activates the *Il17a* and *Il17f* expression found within CCR6⁺IMQ epidermal $\gamma\delta$ T cell subsets. Furthermore, this downstream pathway activation by *Rora* is predicted by IPA Knowledge Base to lead to activation of *Il22* as well as the CCL20/CCR6 axis in CCR6⁺IMQ epidermal $\gamma\delta$ T cell subsets (Fig. 3C). Our results suggest that the activation of the MYC pathway within CCR6⁺IMQ epidermal $\gamma\delta$ T cell subsets contributes to the increased $\gamma\delta$ 17 cytokine profile observed within CCR6⁺IMQ epidermal $\gamma\delta$ T cell subsets.

Psoriasis increases IL-17 and CCR6 production by epidermal $\gamma\delta$ T cells.

To validate the scRNAseq findings that CCR6⁺ epidermal $\gamma\delta$ T cells produce IL-17A during psoriasis, we examined IL-17A production *in vivo* using IL-17A GFP reporter mice. To establish when CCR6 upregulation occurs post-IMQ treatment, a pilot experiment was performed using C57BL/6J wild type mice. Pilot results indicate that CCR6 expression by epidermal $\gamma\delta$ T cells peaks after two days of IMQ treatment. Thus, in our studies, mice received IMQ treatment for two days prior to analysis. This timepoint is similar to previous studies in wound healing models when epidermal $\gamma\delta$ T cell activation was observed within 6 hours of wounding and function persists for at least two days (17, 29). Epidermal sheets were costained for V γ 5, and CCR6, while

IL-17A was detected with GFP, and epidermal $\gamma\delta$ T cells quantified per mm^2 (Fig. 4A). During IMQ-induced psoriasis, there are more IL-17A-producing epidermal $\gamma\delta$ T cells than controls (Fig. 4A, B), but this increase is just short of reaching significance ($p=0.075$) (Fig. 4B). Similarly, there are more CCR6-expressing epidermal $\gamma\delta$ T cells upon IMQ treatment (Fig. 4A, 4B). While CCR6⁺IL-17A⁺ epidermal $\gamma\delta$ T cells were easily identified in IMQ treated mice, the increases that did not reach significance. Similarly, no significant differences were found in the percentage of CCR6⁺ epidermal $\gamma\delta$ T cells that were also IL-17A⁺ (Fig. 4A, 4B). However, given that the epidermal $\gamma\delta$ T cells express both CCR6 and IL17A in a time-dependent manner, CCR6 may be upregulated prior to IL-17A.

IL-17 and CCR6 upregulation by epidermal $\gamma\delta$ T cells in obese and lean mice is similar in psoriasis.

To determine whether there is an impact of obesity on CCR6 expression or IL-17 production by epidermal $\gamma\delta$ T cells in psoriasis-like inflammation, IL-17A GFP reporter mice were fed either a NCD or HFD for 12-16 weeks and then received IMQ treatment for two days. There is a significant increase in IL-17 production by epidermal $\gamma\delta$ T cells within the IMQ group when compared to the control group in mice fed a HFD (Fig. 4A, 4B). This is now significant where it was only reaching significance in the lean control group suggesting a subtle effect of obesity on IL-17 production by epidermal $\gamma\delta$ T cells. Upregulation of CCR6 by epidermal $\gamma\delta$ T cells in psoriasis occurs in both NCD and HFD-fed mice to a similar degree, suggesting obesity does not exacerbate CCR6 expression at this timepoint of IMQ-induced psoriasis onset (Fig. 4A, B).

CCR6 is upregulated within 1 day and downregulated by 3 days post-wounding.

To determine how CCR6 is regulated by epidermal $\gamma\delta$ T cells in response to wounding, we performed a time course. Epidermal $\gamma\delta$ T cells are known to become activated and produce growth factors and cytokines for the first two days post wounding. Thus, we examined CCR6 expression on epidermal $\gamma\delta$ T cells at days 0, 1, 2 and 3 post wounding. As expected, there is little to no CCR6 expression by epidermal $\gamma\delta$ T cells in non-wounded control skin (Fig. 5A,B). However, the number of CCR6 expressing cells increases significantly 1 day post wounding, with CCR6 expression returning to nonwounded control levels 3 days post wounding (Fig. 5A,B). Overall, this data indicates that CCR6 expression by epidermal $\gamma\delta$ T cells is early and temporal during wound repair instead of being constitutive as in dermal $\gamma\delta$ T cells.

IL-17A-expressing epidermal $\gamma\delta$ T cells are significantly increased at the wound site.

CCR6 and IL-17 production by epidermal $\gamma\delta$ T cells were examined in wounded and non-wounded IL-17A reporter mice. IL-17A-producing epidermal $\gamma\delta$ T cells were increased in wounded mice as compared to their non-wounded counterparts. CCR6-expressing epidermal $\gamma\delta$ T cells from wounded NCD mice were increased in two of the three wounded mice as compared to nonwounded mice (Fig. 6A, 6B). 20% of the CCR6⁺ epidermal $\gamma\delta$ T cells express IL-17A in wounded mice compared to 0% in non-wounded mice. Together this data suggests that wounding induces epidermal $\gamma\delta$ T cells to upregulate IL-17 and this occurs on a proportion of CCR6⁺ cells.

Obesity increases IL-17A production and CCR6 expression by epidermal $\gamma\delta$ T cells at the wound site.

Previous studies have shown that obesity alters epidermal $\gamma\delta$ T cell number and function during wound repair (8, 14). To determine if there is a shift in epidermal $\gamma\delta$ T cell function

toward a T $\gamma\delta$ 17 phenotype in obesity IL-17A GFP reporter mice were fed either a NCD or HFD for 12-16 weeks and then were wounded for 1 day prior to analysis. Obese mice exhibit an increase in IL-17A-producing epidermal $\gamma\delta$ T cells in wounded vs non-wounded mice (Fig. 6B). In addition, at the wound site, obese mice exhibit significantly elevated numbers of IL-17A-producing epidermal $\gamma\delta$ T cells as compared to their NCD counterparts (Fig. 6B). CCR6 expression by epidermal $\gamma\delta$ T cells at the wound site is also significantly increased in obese mice as compared to lean mice (Fig. 6A, 6B). The number of CCR6⁺ epidermal $\gamma\delta$ T cells that simultaneously express IL-17A is also higher in obese mice upon wounding and as compared to lean wounded mice (Fig. 6B). There is also an increase in the percentage of CCR6⁺ epidermal $\gamma\delta$ T cells concurrently expressing IL-17A, which is nearly significant in the wounded obese group as compared to the wounded lean group (p=0.057) (Fig. 6B). Together these data show that obesity increases T $\gamma\delta$ 17 epidermal $\gamma\delta$ T cells.

Discussion

Epidermal $\gamma\delta$ T cells exhibit a variety of functional responses including $T\gamma\delta 1$, $T\gamma\delta 2$, and $T\gamma\delta 17$ for roles in wound repair, tumor cytolysis and contact hypersensitivity (15, 17, 30). These functions are regulated via costimulation through receptors such as JAML and CD100 in wound repair and cytokine reception such as IL-1 β in contact hypersensitivity (16, 31). Here we suggest that there are functional subsets of epidermal $\gamma\delta$ T cells with skewed abilities and that these subsets can be increased by environmental factors such as obesity. Previously, epidermal $\gamma\delta$ T cells with IFN- γ and IL-17 secreting abilities were identified, but there are currently no markers to further define these cells and to define whether these are specific subsets or cellular plasticity (16). We show that the expression of CCR6 upon activation defines a subset of epidermal $\gamma\delta$ T cells with $T\gamma\delta 17$ functional capabilities. Thus, chemokines such as CCL20 can direct the function of a distinct epidermal $\gamma\delta$ T cell subset during activation.

It is possible that identifying subsets of epidermal $\gamma\delta$ T cells has been difficult because the markers are more easily observed during activation. Particularly for the CCR6⁺ subset, T cell activation is required for the upregulation of CCR6 and then chemokine reception is required for IL-17A production. Our data suggest that there is a temporal requirement for TCR signaling, followed by CCR6 upregulation and CCL20 reception to get IL-17A production. We reveal an association between the $T\gamma\delta 17$ profile observed in CCR6⁺ epidermal $\gamma\delta$ T cells during psoriasis and the upstream transcription factor Myc. Myc is an early response gene in T cell activation (32). Expression of Myc is regulated by TCR signal strength and cytokine reception such as IL-2 (33). This correlates well with our finding that CCR6⁺ epidermal $\gamma\delta$ T cells also express CD25. Further, we find that Myc activation is positively associated with ROR α , primarily attributed to the inhibition of early growth response protein 2 (EGR2). EGR2 deficiency in CD4 T cells leads

to an increase in IL-17 expression (34). Furthermore, it has been established that the overexpression of Myc by $\gamma\delta$ NKT cells results in EGR2 deficiency (35). Our results are consistent with published studies which indicate ROR α directly regulates the expression of both CCR6 and IL-17 (36). When considering the known interaction between ROR α , EGR2, and Myc, our results suggest that the pathway involving Myc, EGR2, and ROR α may serve as a promising focus for understanding the underlying mechanisms behind the expression of the T $\gamma\delta$ 17 profile in CCR6⁺ epidermal $\gamma\delta$ T cells during skin inflammation.

Obesity increases the number of CCR6 and IL-17-expressing epidermal $\gamma\delta$ T cells during the early stages of wound repair, but not during IMQ-induced psoriasis. It is possible that there is a set number of epidermal $\gamma\delta$ T cells with preprogrammed T $\gamma\delta$ 17 function and that IMQ-induced psoriasis activates the entire subset. Thus, obesity would not induce an additional increase, while wounding only induces some of the T $\gamma\delta$ 17 epidermal T cells and obesity further increases the number of activated T $\gamma\delta$ 17 epidermal T cells. Previous research has demonstrated that obesity not only upregulates IL-17 but also boosts the production of CCL20 (24, 37). This dysregulation of the epidermis corresponds to our previous findings that show the cellular composition and organization of the epidermis is altered in HFD and db/db mouse models of obesity due to hyperglycemia and chronic inflammation. In diabetes and obesity, T cell and keratinocyte numbers and tissue repair functions are compromised. Epidermal $\gamma\delta$ T cell dysfunction plays a role in the reduced number and increased differentiation of keratinocytes in both models (8, 14). Another theory is that obesity does not increase IL-17 and CCR6-expressing epidermal $\gamma\delta$ T cells during psoriasis because of the experimental timeline we used. During IMQ-induced psoriasis, IL-17 production is evident in skin resident T cell populations, and continues to rise throughout

the 7 day IMQ treatment (20). For this study we chose the timepoint in which we observed the most CCR6⁺ epidermal $\gamma\delta$ T cells in lean mice, but obesity may alter that timepoint.

CCR6 has been associated with numerous diseases including psoriasis and is a target for therapeutic intervention, but CCR6 targeting drugs have not yet been approved by the FDA (38, 39). Cells including dermal $\gamma\delta$ T cells utilize CCR6 to traffic to the epidermis during inflammation (21, 40). Thus, drugs that block the function of CCR6 or interaction with CCL20 would reduce the recruitment of IL-17-producing T cells. Epidermal $\gamma\delta$ T cells normally reside in the basal layer between keratinocytes and are not known for migrating within or outside of the epidermis (17, 41). Here we have identified a clear subset of epidermal $\gamma\delta$ T cells that upregulate CCR6 and thus would also be targeted with CCR6-specific therapeutics. It is now clear that CCR6⁺ epidermal $\gamma\delta$ T cells contribute to T $\gamma\delta$ 17-associated responses in psoriasis and wound healing, challenging previous assumptions that other dermal and infiltrating cell types were the only IL-17-producers (13, 25). Further, this data showcases the impact of obesity on epidermal $\gamma\delta$ T cell subsets and function in inflammatory settings.

401 **Acknowledgements:** The authors thank the Jameson lab members for manuscript review.

402

References

1. Abramczyk, R., J. N. Queller, A. W. Rachfal, and S. S. Schwartz. 2020. Diabetes and Psoriasis: Different Sides of the Same Prism. *Diabetes Metab. Syndr. Obes. Targets Ther.* 13: 3571–3577.
2. Brazzelli, V., P. Maffioli, V. Bolcato, C. Ciolfi, A. D'Angelo, C. Tinelli, and G. Derosa. 2021. Psoriasis and Diabetes, a Dangerous Association: Evaluation of Insulin Resistance, Lipid Abnormalities, and Cardiovascular Risk Biomarkers. *Front. Med.* 8: 605691.
3. Loots, M. A., E. N. Lamme, J. R. Mekkes, J. D. Bos, and E. Middelkoop. 1999. Cultured fibroblasts from chronic diabetic wounds on the lower extremity (non-insulin-dependent diabetes mellitus) show disturbed proliferation. *Arch. Dermatol. Res.* 291: 93–99.
4. Evans, E. A., S. R. Sayers, X. Kodji, Y. Xia, M. Shaikh, A. Rizvi, J. Frame, S. D. Brain, M. P. Philpott, R. F. Hannen, and P. W. Caton. 2020. Psoriatic skin inflammation induces a pre-diabetic phenotype via the endocrine actions of skin secretome. *Mol. Metab.* 41: 101047.
5. Sen, C. K. 2021. Human Wound and Its Burden: Updated 2020 Compendium of Estimates. *Adv. Wound Care.* 10: 281–292.
6. Huangfu, L., R. Li, Y. Huang, and S. Wang. 2023. The IL-17 family in diseases: from bench to bedside. *Signal Transduct. Target. Ther.* 8: 1–22.
7. McGeachy, M. J., D. J. Cua, and S. L. Gaffen. 2019. The IL-17 family of cytokines in health and disease. *Immunity* 50: 892.
8. Taylor, K. R., A. E. Costanzo, and J. M. Jameson. 2011. Dysfunctional $\gamma\delta$ T cells contribute to impaired keratinocyte homeostasis in mouse models of obesity. *J. Invest. Dermatol.* 131: 2409.
9. Gray, E. E., F. Ramírez-Valle, Y. Xu, S. Wu, Z. Wu, K. E. Karjalainen, and J. G. Cyster. 2013. IL-17-committed $V\gamma 4+$ $\gamma\delta$ T cell deficiency in a spontaneous Sox13 mutant CD45.1 congenic mouse substrain protects from dermatitis. *Nat. Immunol.* 14: 584–592.
10. Harper, E. G., C. Guo, H. Rizzo, J. V. Lillis, S. E. Kurtz, I. Skorcheva, D. Purdy, E. Fitch, M. Iordanov, and A. Blauvelt. 2009. Th17 Cytokines Stimulate CCL20 Expression in Keratinocytes In Vitro and In Vivo: Implications for Psoriasis Pathogenesis. *J. Invest. Dermatol.* 129: 2175.
11. Zhou, S., Q. Li, H. Wu, and Q. Lu. 2020. The pathogenic role of innate lymphoid cells in autoimmune-related and inflammatory skin diseases. *Cell. Mol. Immunol.* 17: 335.
12. Carolan, E., L. M. Tobin, B. A. Mangan, M. Corrigan, G. Gaoatswe, G. Byrne, J. Geoghegan, D. Cody, J. O'Connell, D. C. Winter, D. G. Doherty, L. Lynch, D. O'Shea, A. E. Hogan. 2015. Altered distribution and increased IL-17 production by mucosal-associated invariant T cells in adult and childhood obesity. *J. Immunol. Baltim. Md 1950* 194: 5775–80.
13. Cai, Y., X. Shen, C. Ding, C. Qi, K. Li, X. Li, V. R. Jala, H. Zhang, T. Wang, J. Zheng, and J. Yan. 2011. Pivotal Role of Dermal IL-17-producing $\gamma\delta$ T Cells in Skin Inflammation. *Immunity* 35: 596.
14. Taylor, K. R., R. E. Mills, A. E. Costanzo, and J. M. Jameson. 2010. $\gamma\delta$ T Cells Are Reduced and Rendered Unresponsive by Hyperglycemia and Chronic TNF α in Mouse Models of Obesity and Metabolic Disease. *PLOS ONE* 5: e11422.
15. Nielsen, M. M., P. Lovato, A. S. MacLeod, D. A. Witherden, L. Skov, B. Dyring-Andersen, S. Dabelsteen, A. Woetmann, N. Ødum, W. L. Havran, C. Geisler, and C. M. Bonefeld. 2014. IL-1 β -dependent activation of dendritic epidermal T cells in contact hypersensitivity. *J. Immunol. Baltim. Md 1950* 192: 2975.
16. MacLeod, A. S., S. Hemmers, O. Garijo, M. Chabod, K. Mowen, D. A. Witherden, and W. L. Havran. 2013. Dendritic epidermal T cells regulate skin antimicrobial barrier function. *J. Clin. Invest.* 123: 4364–4374.

17. Jameson, J., K. Ugarte, N. Chen, P. Yachi, E. Fuchs, R. Boismenu, W. L. Havran. 2002. A role for skin gammadelta T cells in wound repair. *Science* 296: 747–9
18. Sharp L. L., J. Jameson, G. Cauvi, and W. L. Havran. 2005. Dendritic epidermal T cells regulate skin homeostasis through local production of insulin-like growth factor 1. *Nat. Immunol.* 6: 73–9
19. Daniel, T., B. M. Thobe, I.H. Chaudry, M. A. Choudhry, W. J. Hubbard, M. G. Schwacha. 2007. Regulation of the postburn wound inflammatory response by gammadelta T-cells. *Shock Augusta Ga* 28: 278–83
20. Liu, Y., C. Cook, A. J. Sedgewick, S. Zhang, M. S. Fassett, R. R. Ricardo-Gonzalez, P. Harirchian, S. W. Kashem, S. Hanakawa, J. R. Leistico, J. P. North, M. A. Taylor, W. Zhang, M.-Q. Man, A. Charruyer, N. Beliakova-Bethell, S. C. Benz, R. Ghadially, T. M. Mauro, D. H. Kaplan, K. Kabashima, J. Choi, J. S. Song, R. J. Cho, and J. B. Cheng. 2020. Single-Cell Profiling Reveals Divergent, Globally Patterned Immune Responses in Murine Skin Inflammation. *iScience* 23: 101582
21. Mabuchi, T., T. P. Singh, T. Takekoshi, G. Jia, X. Wu, M. C. Kao, I. Weiss, J. M. Farber, and S. T. Hwang. 2013. CCR6 is required for epidermal trafficking of $\gamma\delta$ T cells in an IL-23-induced model of psoriasiform dermatitis. *J. Invest. Dermatol.* 133: 164.
22. Schutyser, E., S. Struyf, J. Van Damme. 2003. The CC chemokine CCL20 and its receptor CCR6. *Cytokine Growth Factor Rev.* 14: 409–26
23. Anderson, L. S., S. Yu, K. R. Rivara, M. B. Reynolds, A. A. Hernandez, X. Wu, H.-Y. Yang, R. R. Isseroff, L. S. Miller, S. T. Hwang, and S. I. Simon. 2019. CCR6+ $\gamma\delta$ T cells home to skin wounds and restore normal wound healing in CCR6-deficient mice. *J. Invest. Dermatol.* 139: 2061.
24. Wu, C., X. Chen, J. Shu, and C.-T. Lee. 2017. Whole-genome expression analyses of type 2 diabetes in human skin reveal altered immune function and burden of infection. *Oncotarget* 8: 34601.
25. Gray, E. E., K. Suzuki, and J. G. Cyster. 2011. Identification of a motile IL-17 producing $\gamma\delta$ T cell population in the dermis. *J. Immunol. Baltim. Md 1950* 186: 6091.
26. Gargas, S., S. Bshara-Corson, M. Cruz, J. Jameson. 2019. Isolation and Analysis of Mouse and Human Skin $\gamma\delta$ T Cells. *Curr. Protoc. Immunol.* 127: e92
27. Tan, L., I. Sandroek, I. Odak, Y. Aizenbud, A. Wilharm, J. Barros-Martins, Y. Tabib, A. Borchers, T. Amado, L. Gangoda, M. J. Herold, M. Schmidt-Supprian, J. Kisielow, B. Silva-Santos, C. Koenecke, A.-H. Hovav, C. Krebs, I. Prinz, and S. Ravens. 2019. Single-Cell Transcriptomics Identifies the Adaptation of Scart1+ V γ 6+ T Cells to Skin Residency as Activated Effector Cells. *Cell Rep.* 27: 3657-3671.e4.
28. Chi, X., W. Jin, X. Bai, and C. Dong. 2021. ROR α is critical for mTORC1 activity in T cell-mediated colitis. *Cell Rep.* 36: 109682.
29. Komori, H. K., D.A. Witherden, R. Kelly, K. Sendaydiego, J. M. Jameson, L. Teyton, W. L. Havran. 2012. Cutting edge: dendritic epidermal $\gamma\delta$ T cell ligands are rapidly and locally expressed by keratinocytes following cutaneous wounding. *J. Immunol. Baltim. Md 1950* 188: 2972–6
30. Girardi, M., D. E. Oppenheim, C. R. Steele, J. M. Lewis, E. Glusac, R. Filler, P. Hobby, B. Sutton, R. E. Tigelaar, A. C. Hayday. 2001. Regulation of cutaneous malignancy by gammadelta T cells. *Science* 294: 605–9
31. Nielsen, M. M., D. A. Witherden, and W. L. Havran. 2017. $\gamma\delta$ T cells in homeostasis and host defence of epithelial barrier tissues. *Nat. Rev. Immunol.* 17: 733–745.

32. Nie, Z., G. Hu, G. Wei, K. Cui, A. Yamane, W. Resch, R. Wang, D. R. Green, L. Tessarollo, R. Casellas, K. Zhao, D. Levens. 2012. c-Myc is a universal amplifier of expressed genes in lymphocytes and embryonic stem cells. *Cell* 151: 68–79
33. Preston, G. C., L. V. Sinclair, A. Kaskar, J. L. Hukelmann, M. N. Navarro, I. Ferrero, H. R. MacDonald, V. H. Cowling, and D. A. Cantrell. 2015. Single cell tuning of Myc expression by antigen receptor signal strength and interleukin-2 in T lymphocytes. *EMBO J.* 34: 2008–24
34. Zhu, B., A. L. J. Symonds, J. E. Martin, D. Kioussis, D. C. Wraith, S. Li, and P. Wang. 2008. Early growth response gene 2 (Egr-2) controls the self-tolerance of T cells and prevents the development of lupus like autoimmune disease. *J. Exp. Med.* 205: 2295–2307.
35. Zhang, B., A. Jiao, M. Dai, D. L. Wiest, and Y. Zhuang. 2018. Id3 restricts $\gamma\delta$ NKT cell expansion by controlling Egr2 and c-Myc activity. *J. Immunol. Baltim. Md 1950* 201: 1452.
36. Wang, R., S. Campbell, M. Amir, S. A. Mosure, M. A. Bassette, A. Eliason, M. S. Sundrud, T. M. Kamenecka, and L. A. Solt. 2021. Genetic and pharmacological inhibition of the nuclear receptor ROR α regulates TH17 driven inflammatory disorders. *Nat. Commun.* 12: 1–18.
37. Liu, Z., Y. Xu, L. Chen, J. Xie, J. Tang, J. Zhao, B. Shu, S. Qi, J. Chen, G. Liang, G. Luo, J. Wu, W. He, X. Liu. 2016. Dendritic epidermal T cells facilitate wound healing in diabetic mice. *Am. J. Transl. Res.* 8: 2375–84
38. Rees, P. A., N. S. Greaves, M. Baguneid, A. Bayat. 2015. Chemokines in Wound Healing and as Potential Therapeutic Targets for Reducing Cutaneous Scarring. *Adv. Wound Care* 4: 687–703
39. Gómez-Melero, S., and J. Caballero-Villarraso. 2023. CCR6 as a Potential Target for Therapeutic Antibodies for the Treatment of Inflammatory Diseases. *Antibodies* 12: 30
40. Liu, Z., Y. Xu, X. Zhang, G. Liang, L. Chen, J. Xie, J. Tang, J. Zhao, B. Shu, S. Qi, J. Chen, G. Luo, J. Wu, W. He, X. Liu. 2016. Defects in dermal V γ 4 $\gamma\delta$ T cells result in delayed wound healing in diabetic mice. *Am. J. Transl. Res.* 8: 2667–80
41. Chodaczek, G., M. Toporkiewicz, M. A. Zal, and T. Zal. 2018. Epidermal T Cell Dendrites Serve as Conduits for Bidirectional Trafficking of Granular Cargo. *Front. Immunol.* 9: 1430

524 Figure Legends:

525 **Figure 1. CCR6 is upregulated by a subset of CD25⁺ epidermal $\gamma\delta$ T cells upon anti-CD3**
 526 **stimulation.** (A) Flow cytometric analysis of epidermal cells isolated from B6 mice, cultured for
 527 9-15 weeks (> 95% epidermal $\gamma\delta$ T cells), and stimulated with anti-CD3. Live, $\gamma\delta$ TCR⁺ cells are
 528 gated and CCR6 and CD25 analyzed (n=3). (B) Flow cytometric analysis of epidermal V γ 5 T
 529 cells stimulated in the presence or absence of anti-CD3 and/or CCL20 for 6 hours. Live, V γ 5⁺ T
 530 cells are gated and TNF- α and IL-17A analyzed (n=3). Data represents the mean +/- SD. * p < .05
 531 and ** p < .01

532 **Figure 2. CCR6⁺ epidermal $\gamma\delta$ T cells exhibit a T $\gamma\delta$ 17 gene expression profile.** Using
 533 publicly available scRNA-Seq data (20) the total skin cell population (n=18,040) was filtered to
 534 epidermal $\gamma\delta$ T cells (n=236). (A) UMAP plot showing epidermal $\gamma\delta$ T cells can be identified in
 535 three distinct clusters. Based on treatment group and CCR6 expression epidermal $\gamma\delta$ T cells were
 536 clustered further into CCR6⁺IMQ, CCR6⁺control, CCR6⁻IMQ, CCR6⁻control. In the treatment
 537 group, the ratio of CCR6⁺ to CCR6⁻ cells increased from 1/48 in the control group to 1/9. (B)
 538 Differential gene expression between 4 different epidermal $\gamma\delta$ T cell populations within
 539 treatment groups displayed in a heatmap (C) Dual heatmap rendering of differential gene
 540 expression between specific epidermal $\gamma\delta$ T cell groups.

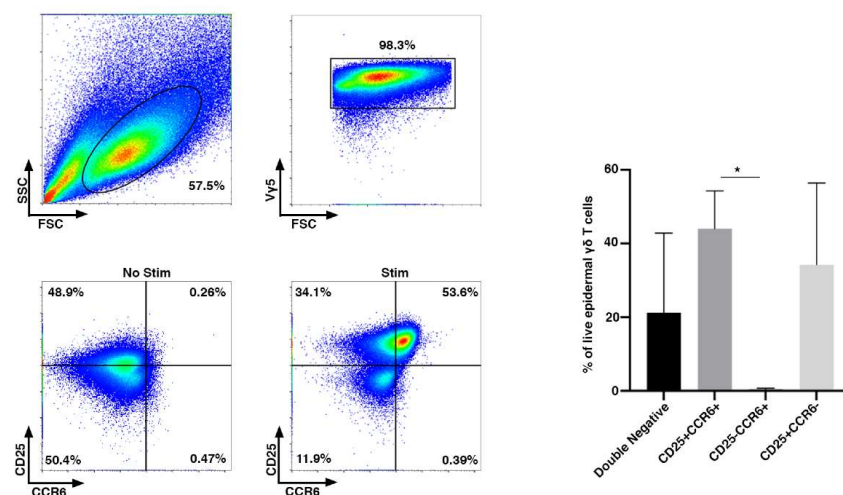
541 **Figure 3. Canonical pathway analysis of differentially expressed genes from CCR6⁺ and**
 542 **CCR6⁻ epidermal $\gamma\delta$ T cells during IMQ-induced psoriasis identify Myc pathway.** (A) Top
 543 differentially expressed genes between CCR6⁺IMQ and CCR6⁻IMQ from publicly available
 544 scRNA sequencing data (20) were clustered into canonical pathways using IPA Knowledge Base
 545 platform. Positive z-score (orange) shows pathway activation. A negative z-score (blue) shows
 546 the pathway is inhibited. No z-score (white) shows the pathway is neither activated nor inhibited.
 547 Bars are arranged by statistical significance. (B) Network analysis identifies upstream regulator
 548 Myc (orange indicating activation), with IPA Knowledge Base predicting a linked activation
 549 with Rora. (C) Network downstream analysis of Rora pathway with orange predicting activation,
 550 blue predicting inhibition, and red predicting an increased measurement between subsets
 551 (CCR6⁺IMQ vs. CCR6⁻IMQ epidermal $\gamma\delta$ T cells).

552 **Figure 4. IMQ-induced psoriasis increases IL-17A and CCR6 expression by epidermal $\gamma\delta$ T**
 553 **cells, while obesity does not further increase expression.** (A) Representative
 554 immunofluorescent images of epidermal sheets from C57BL/6-Il17atm1Bcgen/J mice treated
 555 with and without IMQ for two days. Scale bars, 100 μ m. (B) Quantification of IL-17A⁺, CCR6⁺,
 556 and IL-17A⁺CCR6⁺ epidermal $\gamma\delta$ T cells with and without IMQ treatment (n=3 mice/group). A
 557 minimum of seven fields of view for each mouse were used for analysis and then averaged to
 558 form one data point. * p < 0.05

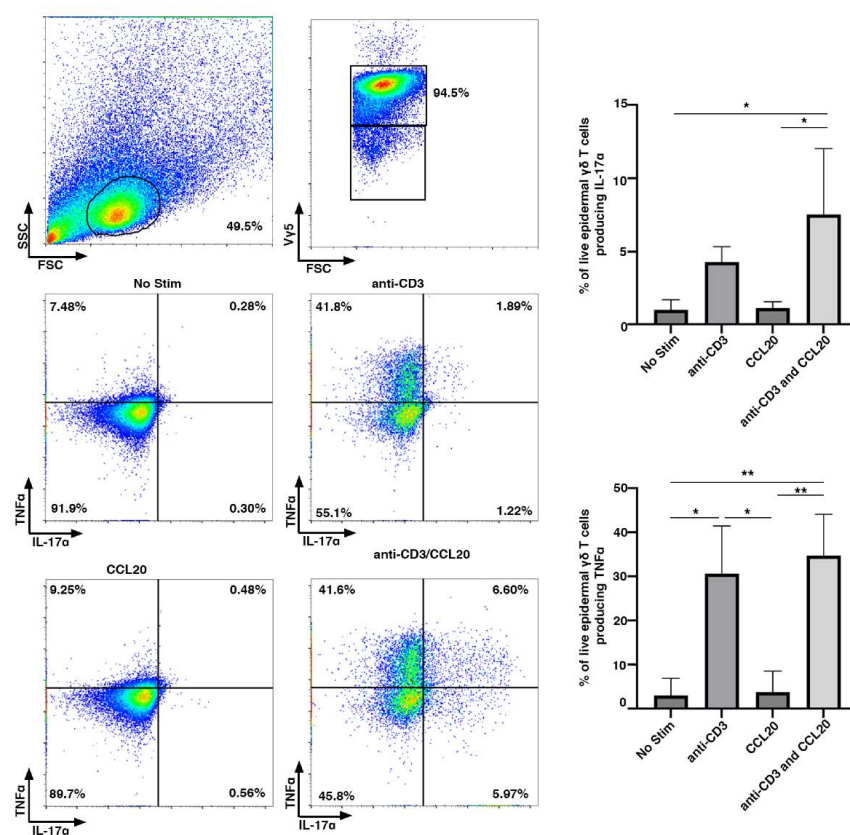
559 **Figure 5. CCR6 is upregulated within the first 24 hrs. post-wounding and downregulated**
 560 **by 72 hrs. post-wounding.** (A) Representative immunofluorescent images of epidermal sheets
 561 from B6 mice at various timepoints post wounding. Wound site indicated with dotted line. Scale
 562 bars, 100 μ m. (B) Quantification of CCR6⁺ epidermal $\gamma\delta$ T cells at different timepoints post
 563 wounding (n= 3-4 mice/group). A minimum of seven fields of view for each mouse were used
 564 for analysis and then averaged to form one data point. p = .05

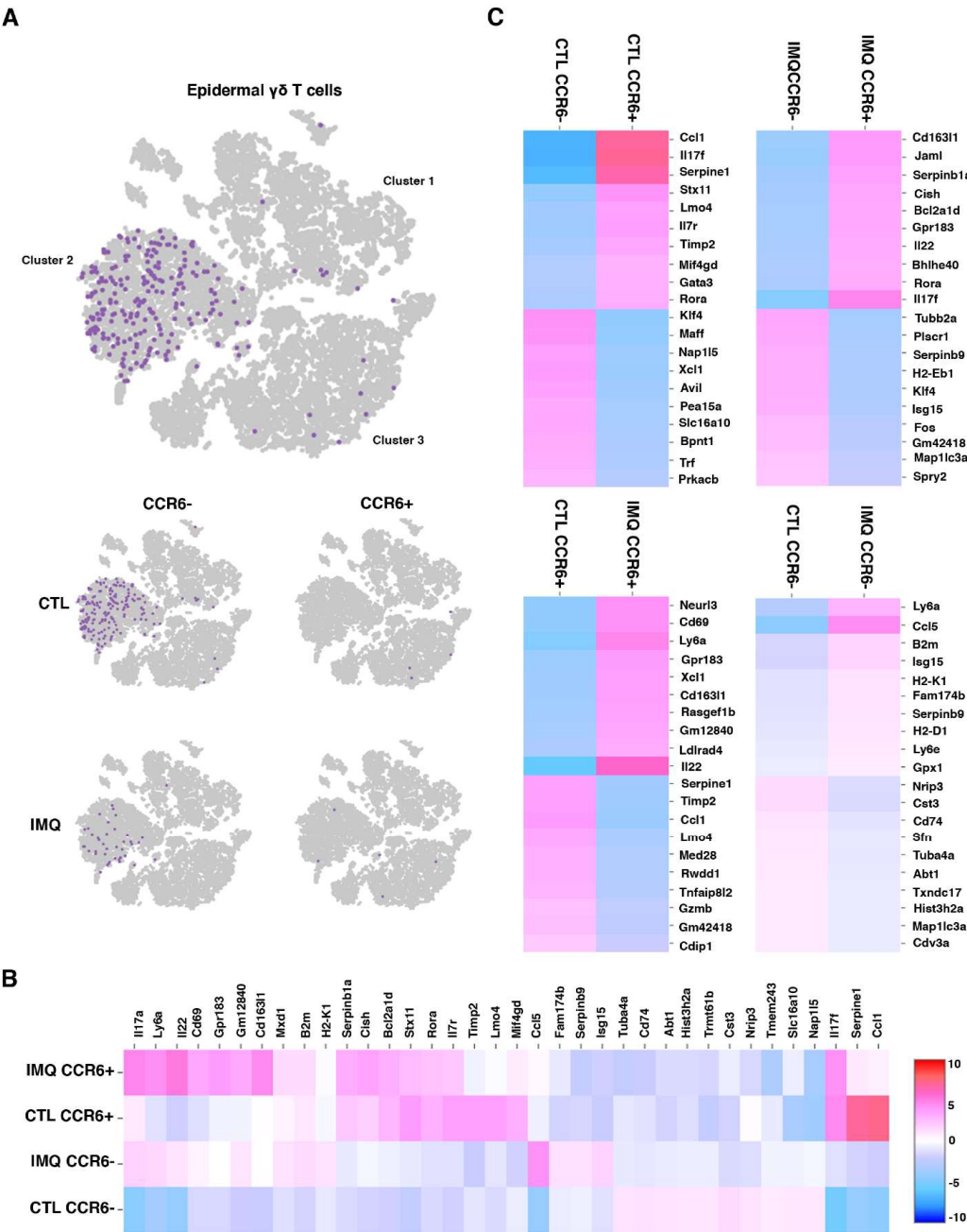
Figure 6. IL-17A and CCR6 expression by epidermal $\gamma\delta$ T cells is significantly elevated in wounded mice, while obesity increases IL-17A production and CCR6 expression by epidermal $\gamma\delta$ T cells at the wound site. (A) Representative immunofluorescent images of epidermal sheets from C57BL/6-Il17atm1Bcgen/J mice one day post wounding. Wound site indicated with dotted line. Scale bars, 100 μ m. **(B)** Quantification of IL-17A⁺, CCR6⁺, and IL-17A⁺CCR6⁺ epidermal $\gamma\delta$ T cells with and without wounding (n=3 mice/group). A minimum of seven fields of view for each mouse were used for analysis and then averaged to form one data point. * $p < 0.05$, ** $p < .01$, *** $p < .001$

A

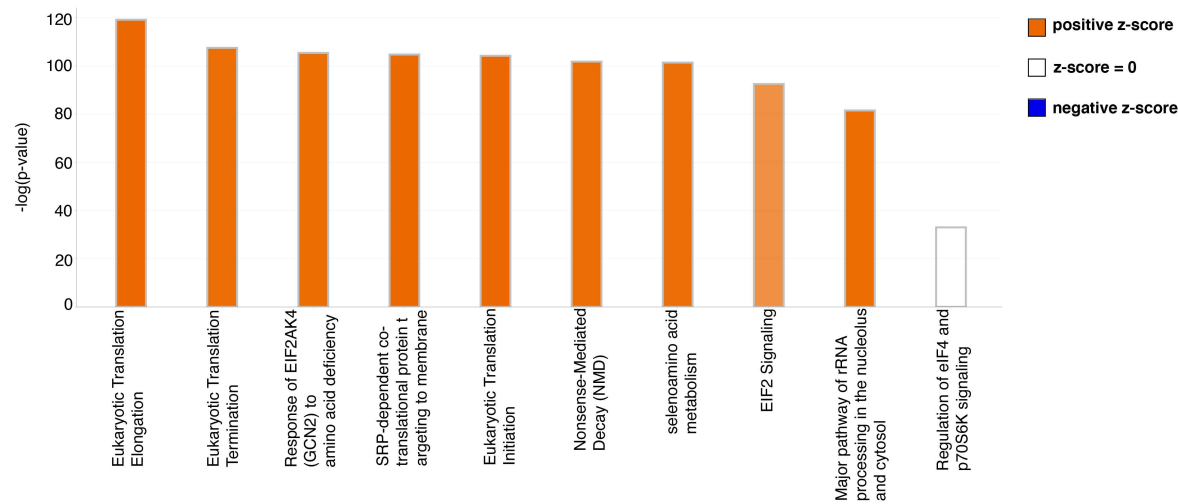


B

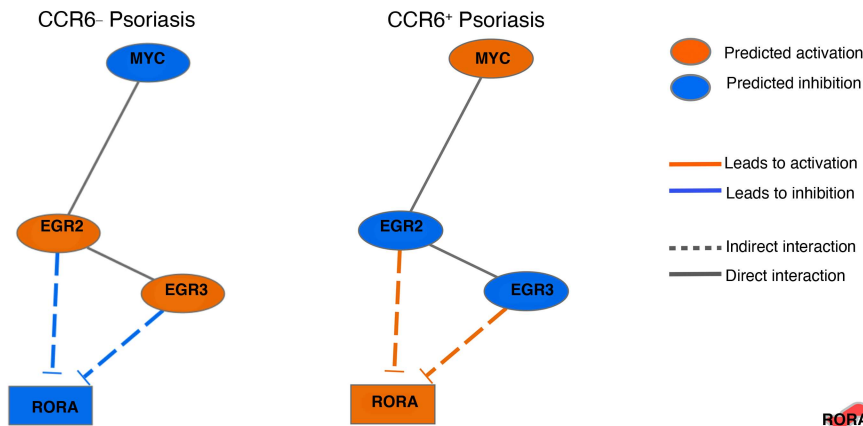




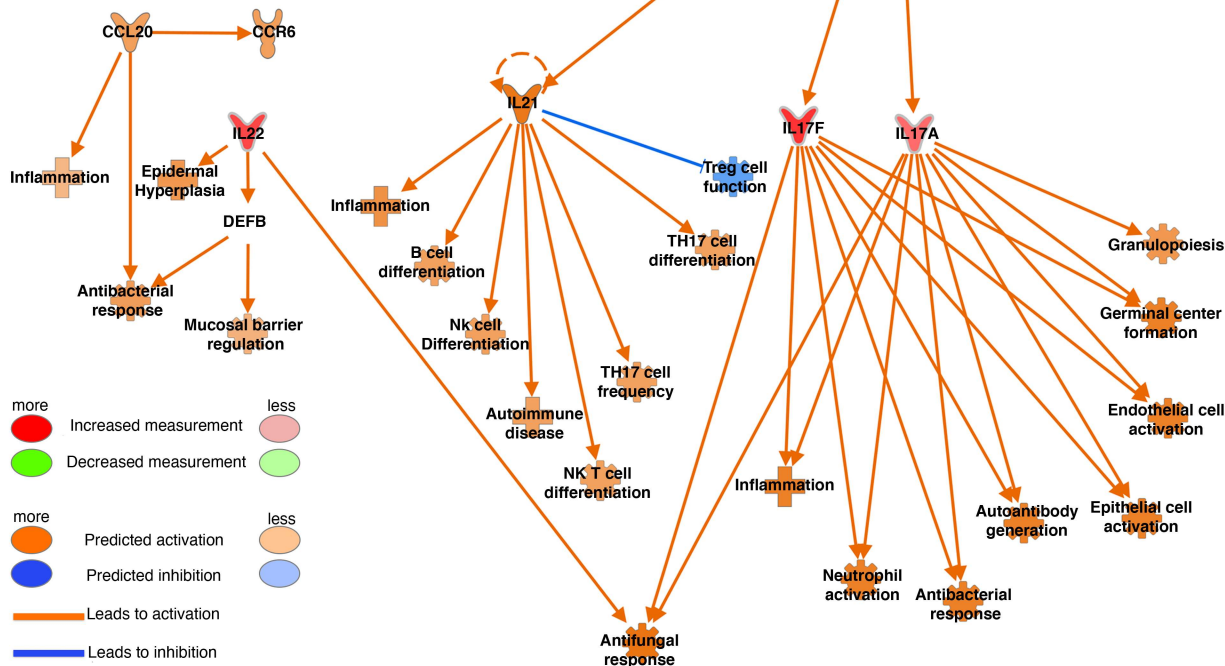
A



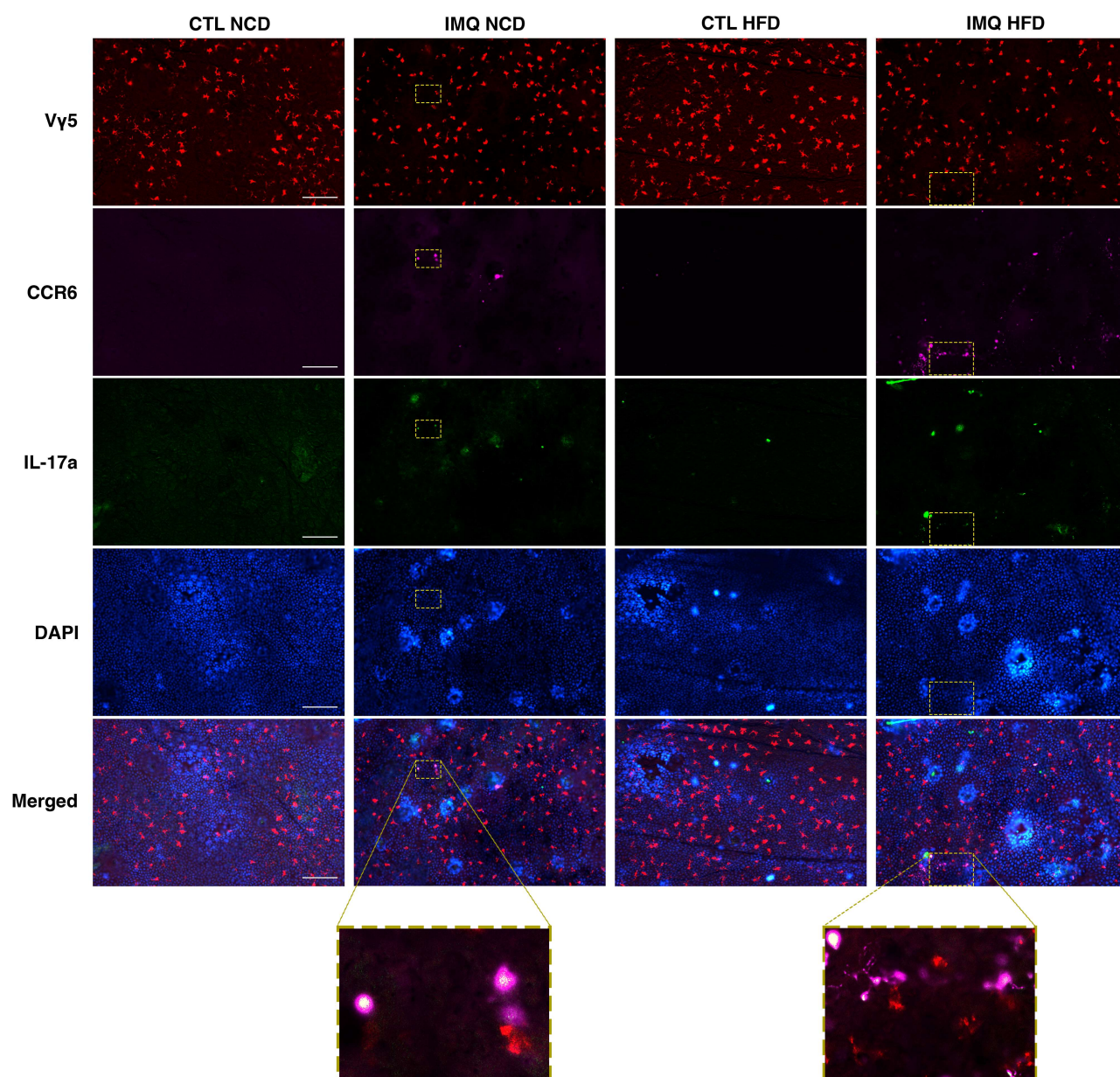
B



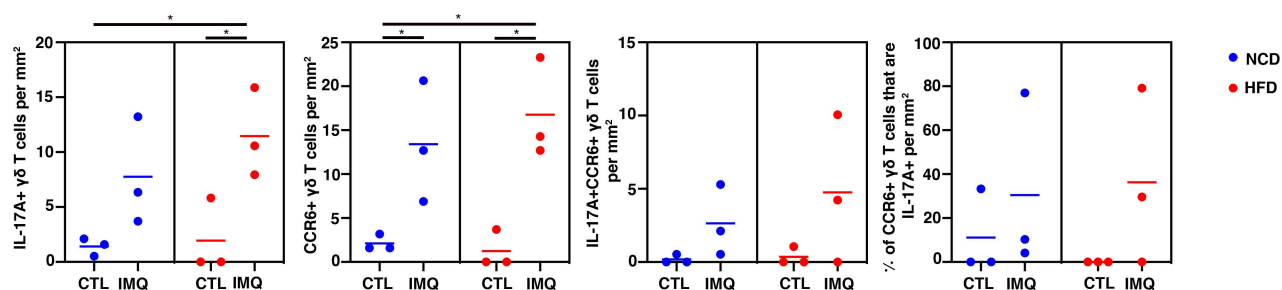
C

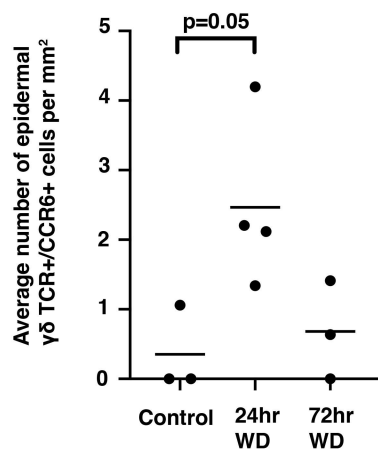


A

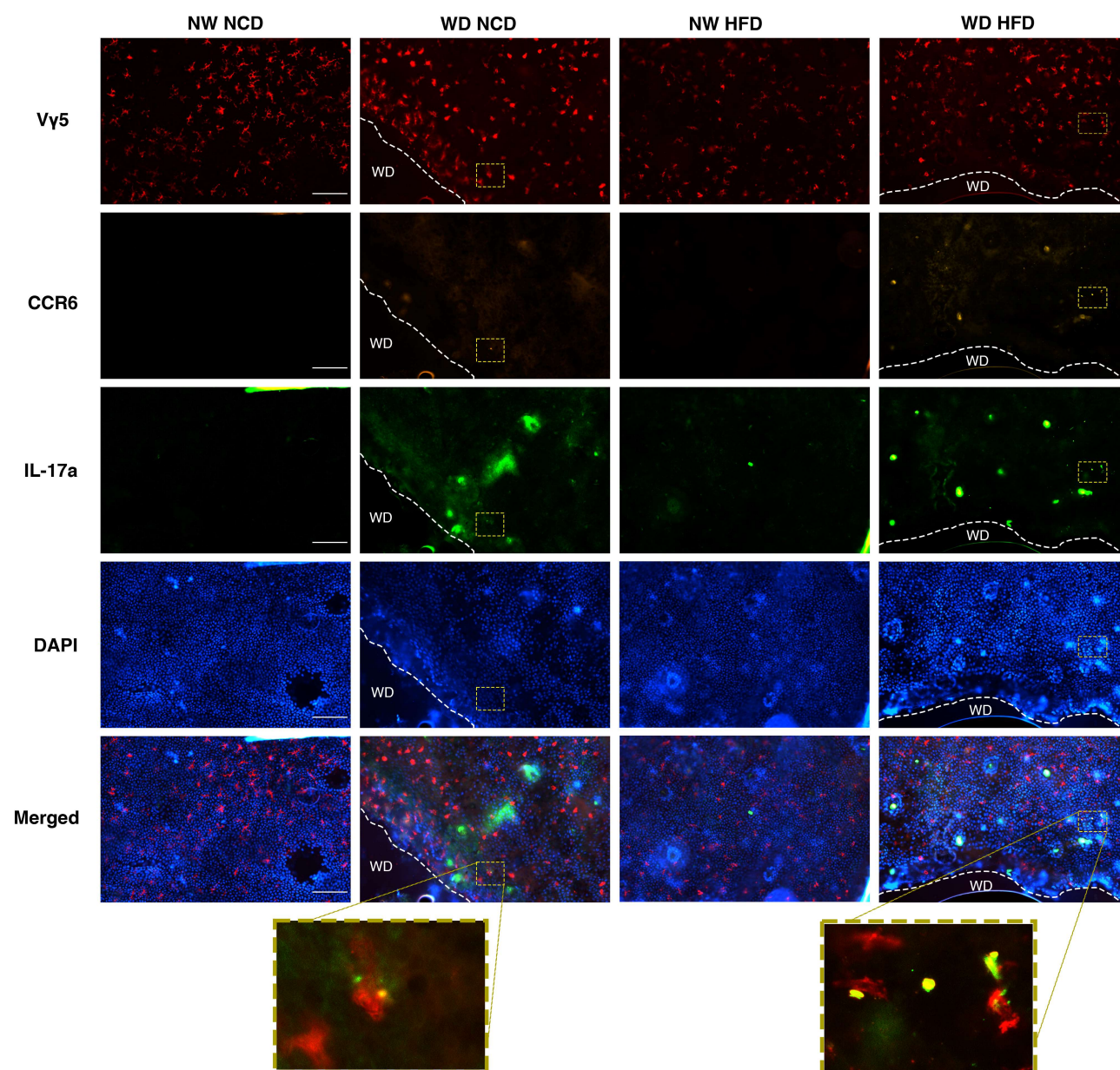


B





A



B

